Original Paper

Cellular Physiology and Biochemistry

Cell Physiol Biochem 2011;28:435-450

Accepted: September 19, 2011

Pendrin Function and Regulation in *Xenopus* Oocytes

Fabian R. Reimold[1,2,*], John F. Heneghan[1,2,*], Andrew K. Stewart[1,2], Israel Zelikovic[3,4,5], David H. Vandorpe[1,2], Boris E. Shmukler[1,2] and Seth L. Alper[1,2]

[1]Renal Division and Molecular and Vascular Medicine Unit, Beth Israel Deaconess Medical Center [2]Department of Medicine, Harvard Medical School, Boston, [3]Laboratory of Developmental Nephrology, Dept. of Physiology and Biophysics, Faculty of Medicine, [4]The Rappaport Family Institute for Research in the Medical Sciences, Technion-Israel Institute of Technology, [5]Division of Pediatric Nephrology, Rambam Medical Center, Haifa, *equal contributions

Key Words

Iodide • Bromide • Chloride • Formate • *Xenopus* oocyte • Methanethiosulfonate • Phorbol ester • Protein kinase C δ

Abstract

SLC26A4/PDS mutations cause Pendred Syndrome and non-syndromic deafness. but some aspects of function and regulation of the *SLC26A4* polypeptide gene product, pendrin, remain controversial or incompletely understood. We have therefore extended the functional analysis of wildtype and mutant pendrin in *Xenopus* oocytes, with studies of isotopic flux, electrophysiology, and protein localization. Pendrin mediated electroneutral, pH-insensitive, DIDS-insensitive anion exchange, with extracellular $K_{(1/2)}$ (in mM) of 1.9 (Cl^-), 1.8 (I^-), and 0.9 (Br^-). The unusual phenotype of Pendred Syndrome mutation E303Q (loss-of-function with normal surface expression) prompted systematic mutagenesis at position 303. Only mutant E303K exhibited loss-of-function unrescued by forced overexpression. Mutant E303C was insensitive to charge modification by methanethiosulfonates. The corresponding mutants SLC26A2 E336Q, SLC26A3 E293Q, and SLC26A6 E298Q exhibited similar loss-of-function phenotypes, with wildtype surface expression also documented for SLC26A2 E336Q. The strong inhibition of wildtype SLC26A2, SLC26A3, and SLC26A6 by phorbol ester contrasts with its modest inhibition of pendrin. Phorbol ester inhibition of SLC26A2, SLC26A3, and SLC26A6 was blocked by coexpressed kinase-dead PKCδ but was without effect on pendrin. Mutation of SLC26A2 serine residues conserved in PKCδ -sensitive SLC26 proteins but absent from pendrin failed to reduce PKCδ sensitivity of SLC26A2 (190).

Copyright © 2011 S. Karger AG, Basel

Introduction

Pendrin is the polypeptide product of the *SLC26A4/PDS* gene. Pendrin mediates anion exchange, with physiological specificity encompassing chloride, bicarbonate, iodide, and formate. Mutations in the *SLC26A4* gene cause nonsyndromic deafness with enlargement of the vestibular aqueduct (EVA; DFNB4) as well as Pendred Syndrome, in which deafness is accompanied by defective thyroid iodide organification

KARGER

Fax +41 61 306 12 34
E-Mail karger@karger.ch
www.karger.com

© 2011 S. Karger AG, Basel
1015-8987/11/0283-0435$38.00/0

Accessible online at:
www.karger.com/cpb

Seth L. Alper, MD, PhD
Beth Israel Deaconess Medical Center RN-380F
99 Brookline Ave, Boston, MA 02215 (USA)
Tel. +1 617-667-2930, Fax +1 617-667-0445
E-Mail salper@bidmc.harvard.edu

evident as an elevated perchlorate discharge test, and incompletely penetrant, often euthyroid goiter [1, 2]. More than 200 *SLC26A4* mutations have been catalogued in association with one of these two clinical entities [3, 4]. Among the pendrin missense mutant polypeptides that have been investigated, most are retained inside the cell, likely due to misfolding.

In the cochlea, pendrin is expressed in the epithelial cells of the spiral prominence, root cells, and spindle cells of the stria vascularis. In the vestibular apparatus, pendrin is expressed in nonsensory epithelial cells surrounding sensory hair-cell patches in the saccule, utricle, and ampulla, and in a subset of cells of the endolymphatic sac terminating the vestibular aqueduct [5]. Lack of pendrin-mediated Cl^-/HCO_3^- exchange in the inner ear acidifies endolymph, thus promoting loss of the endocochlear potential and elevating endolymph $[Ca^{2+}]$ [6, 7], and likely contributes to enlargement of the cochlear lumen [8] and vestibular aqueduct through reduced volume absorption. Development of normal hearing in the mouse requires pendrin expression between e16.5 and p2 of embryonic and neonatal developent [5].

Pendrin is also expressed in the apical membrane of the thyrocyte, where it likely mediates Cl^-/I^- exchange across the thyrocyte apical membrane, contributing to iodide uptake and organification in the lumen of the thyroid follicle [9]. However, loss of pendrin function is often unaccompanied by any thyroid phenotype in both humans and mice, and the importance of pendrin to thyroid follicular iodide secretion remains mysterious, while additional apical thyrocyte iodide transporters remain unidentified. The possible importance of pendrin-mediated I^-/Cl^- or I^-/HCO_3^- exchange in inner ear development or function also remains unknown.

Pendrin expressed in the apical membrane of non-A intercalated cells of the renal cortical collecting duct [10] mediates Cl^-/HCO_3^- exchange. This major transcellular pathway for Cl^- reabsorption and HCO_3^- secretion is coupled with the Na^+ uptake pathway mediated by Slc4a8 [11], and is regulated by aldosterone, acid and alkaline pH [12], uroguanylin [13], and the alkaline pH-sensitive insulin receptor-related receptor [14].

Pendrin-mediated Cl^-/HCO_3^- exchange in the mouse kidney cortical collecting duct (CCD) contributes to mineralocorticoid and high-salt-induced hypertension [15] and regulates ENaC activity [16], while pendrin-mediated Cl^-/I^- exchange mediates an important component of renal iodide reabsorption [17]. Although human pendrin deficiency generally lacks any clinical renal phenotype, two cases of acute metabolic alkalosis in the setting of acute precipitating illnesses have been reported in Pendred patients [18]. Pendrin has also been proposed to mediate Cl^-/HCO_3^- exchange and SCN^-/Cl^- exchange in interleukin-stimulated airway epithelial cells [19], functions postulated to contribute to asthma pathology or adaptation [20]. Pendrin has also been detected in prolactin-stimulated mammary epithelial cells [21, 22] and regulates iodide secretion in submandibular duct of the mouse salivary gland [23].

Aspects of anion selectivity and acute regulation of pendrin remain controversial or little studied. The physiological consequences of disease-associated mutations unassociated with trafficking abnormalities are similarly understudied. In this paper we address the anion selectivity and physiological regulation of pendrin as expressed in *Xenopus* oocytes, and explore with directed mutagenesis the role of pendrin residue E303, site of the deafness-associated loss-of-function mutation E303Q associated with normal intracellular trafficking [4]. In addition we re-evaluate the mechanism by which protein kinase C regulates SLC26 anion exchangers, and test a hypothesis addressing the distinct PKC response of pendrin compared to other disease-associated SLC26 anion exchangers.

Materials and Methods

Materials

$Na^{36}Cl$ and $Na_2{}^{35}SO_4$ were from ICN (Irvine, CA). ^{14}C-oxalate (NEN-DuPont) was the gift of C. Scheid and T. Honeyman (Univ. Mass. Med. Ctr.). Restriction enzymes were from New England Biolabs (Beverly, MA). T4 DNA ligase and the EXPAND High-fidelity PCR System were from Roche Diagnostics (Indianapolis, IN). 4,4'-diisothiocyanostilbene-2,2'-disulfonic acid (DIDS) was from Calbiochem (La Jolla, CA). (2-aminoethyl)methanethiosulfonate hydrobromide (MTSEA), [(2-trimethylammonium)ethyl]methanethiosulfonate bromide (MTSET), and sodium (2-sulfonatoethyl)methanethiosulfonate (MTSES) were from Toronto Research Biochemicals (Toronto, Ontario). 4β-phorbol-12-myristate-13-acetate (PMA) was from LC Laboratories (Woburn, MA). All other chemical reagents were from Sigma (St. Louis, MO) or Fluka (Milwaukee, WI) and were of reagent grade.

Solutions

Modified Barth's solution (MBS) consisted of (in mM) 88 NaCl, 1 KCl, 2.4 $NaHCO_3$, 0.82 $MgSO_4$, 0.33 $Ca(NO_3)_2$, 0.41 $CaCl_2$, and 10 HEPES (pH adjusted to 7.40 with NaOH). ND-96 (pH 7.40) consisted of (in mM) 96 NaCl, 2 KCl, 1.8 $CaCl_2$, 1 $MgCl_2$, and 5 HEPES, with total $[Cl^-]$ of 103.6 mM. In Cl^--free ND-96 or solutions in which Cl^- was partially substituted with the indicated anions (I^-, Br^-, F^-, NO_3^-, SCN^-), partial Cl^- substitution solutions, NaCl was replaced mole-for-mole with sodium

cyclamate or, in the case of two-electrode voltage clamp experiments, sodium gluconate. In some experiments, 1 mM Na_2SO_4 was added to ND-96, or 30 mM NaCl was replaced with 20 mM Na_2SO_4 as indicated. Cl^- salts of K^+, Ca^{2+}, and Mg^{2+} were substituted on an equimolar basis with the corresponding gluconate salts as needed. Oxalate-containing bath solutions were nominally Ca^{2+}- and Mg^{2+}-free. Addition of the weak acid sodium butyrate (40 mM) to the flux media was in equimolar substitution for sodium cyclamate. Bath addition of NH_4Cl (20 mM) was in equimolar substitution for NaCl.

Mutagenesis of cDNA expression plasmids

Oocyte expression plasmids encoding human pendrin/SLC26A4 and its mutant E303Q [4], human SLC26A2/DTDST (hSCL26A2) [24], hSLC26A3/DRA [25], hSLC26A6 and mSlc26a6 [26] were previously described. The multiple pendrin E303 mutants, hSLC26A3 mutant E293Q, hSLC26A6 mutant E298Q, hSLC26A2 mutant E336Q and double mutant S245V/S249A were each generated by four-primer polymerase chain reaction (PCR) mutagenesis as described [27] (oligonucleotide sequences available upon request). PCR-synthesized products and ligation junctions were sequenced in the final plasmids in entirety to ensure absence of PCR-generated mutations. Mouse protein kinase C-δ (PKCδ) [28] kinase-dead variant K376A [29] in pcDL-Srα296 [30] was the gift of A. Toker (Beth Israel Deaconess Med. Ctr.) The kinase-dead PKCδ open reading frame was subcloned into pXT7.

Expression of cRNAs in Xenopus oocytes

Capped cRNA was transcribed from linearized cDNA templates with the T7 or SP6 Megascript Kit (Ambion, Austin, TX) and purified with the RNeasy mini-kit (Qiagen). cRNA concentration (A_{260}) was measured by Nanodrop spectrometer (ThermoFisher), and integrity was confirmed by formaldehyde agarose gel electrophoresis. Mature female *Xenopus* (Dept. of Systems Biology, Harvard Medical School; or NASCO, Madison, WI) were maintained and subjected to partial ovariectomy under hypothermic tricaine anesthesia following protocols approved by the Institutional Animal Care and Use Committee of Beth Israel Deaconess Medical Center. Stage V-VI oocytes were prepared by overnight incubation of ovarian fragments in MBS with 1.5 mg/ml collagenase B (Roche, Indianapolis, IN), followed by a 20 min rinse in Ca^{2+}-free MBS with subsequent manual selection and defolliculation as needed. Oocytes were injected on the same day with cRNA (0.5-50 ng) or with water in a volume of 50 nl. Injected and uninjected oocytes were then maintained before use for 2-6 days at 17.5°C in MBS containing gentamicin.

Isotopic influx experiments

Unidirectional $^{36}Cl^-$ influx studies were carried out for periods of 15 or 30 min in ND-96 with total bath $[Cl^-]$ of 103.6 mM (0.5 μCi/well). The influx medium was supplemented with 10 μM bumetanide. Some oocytes were preincubated for 15 min at room temperature in Cl^--free solution containing either 2-aminoethyl methanethiosulfonate hydrobromide (MTSEA, 5 mM), sodium 2-sulfonatoethyl methanethiosulfonate (MTSES, 10 mM), or [2-(trimethylammonium)ethyl] methanethiosulfonate bromide (MTSET, 1 mM) [31]. The 30 min $^{36}Cl^-$ influx assay was then carried out in the continued presence of MTS reagents. $^{35}SO_4^{2-}$ influx studies were carried out for 30 min in baths containing (in mM) 1 or 20

$Na_2{}^{35}SO_4$ (2 μCi/150 μL in a microtiter plate well) , 94.5 or 74.5 sodium cyclamate, 2 potassium glutamate, 1.8 calcium glutamate, 1 magnesium glutamate and 5 HEPES [24]. ^{14}C-oxalate influx studies were carried out for 30 min periods in nominally Ca^{2+}- and Mg^{2+}-free influx medium containing (in mM) 96 mM sodi cyclamate, 2 potassium glutamate, 5 HEPES, pH 7.40, with added 1.0 mM sodium oxalate (0.375 μCi/well; 150 μL). Influx experiments were terminated with four washes in ice-cold Cl^--free ND-96, followed by oocyte lysis in 150 μl of 2% sodium dodecyl sulfate (SDS). Duplicate 10 μL aliquots of influx solution were used to calculate specific acitivity of radiolabeled substrate anions. Oocyte anion uptake was calculated from oocyte cpm and bath specific activity.

Isotopic efflux experiments

For unidirectional $^{36}Cl^-$ efflux studies individual oocytes in Cl^--free ND-96 were injected with 50 nl of 260 mM $Na^{36}Cl$ (20,000-24,000 cpm). Following a 5-10 min recovery period in Cl^--free ND-96, the efflux assay was initiated by transfer of individual oocytes to 6 ml borosilicate glass tubes, each containing 1 ml efflux solution. At intervals of 1 or 3 min, 0.95 ml of this efflux solution was removed for scintillation counting and replaced with an equal volume of fresh efflux solution. Following completion of the assay with a final efflux period either in Cl^--free cyclamate solution or in the presence of the inhibitor DIDS (500 μM), each oocyte was lysed in 150 μl of 2% SDS. Samples were counted for 3-5 min such that the magnitude of 2SD was <5% of the sample means.

For ^{14}C-oxalate efflux assays, oocytes were injected with 50 nl of 50 mM Na ^{14}C-oxalate (6000-8000 cpm, with final estimated intracellular concentration 5 mM). Following a recovery period of at least 20 min, efflux was measured in nominally Ca^{2+}-free baths of 103.6 mM NaCl.

To vary pH_i at constant pH_o, oocytes were pre-exposed to 40 mM sodium butyrate (substituting for sodium cyclamate) for 30 min prior to initiation of an efflux experiment to produce intracellular acidification to pH_i 6.8 [32]. Upon removal of bath butyrate (with substitution by sodium cyclamate) during the course of the efflux experiment, pH_i rapidly alkalinized back towards initial pH_i while pH_o remained constant. Variation of pH_o was achieved at near-constant pH_i [33]. Some oocyte groups were exposed to 20 mM NH_4Cl during the course of efflux experiments, acidifying pH_i to 6.9 [34]. Drugs were added to the bath prior to or together with isotope as indicated.

Efflux data were plotted as the natural logarithm (ln) of the quantity (% cpm remaining in the oocyte) vs. time. Efflux rate constants for $^{35}SO_4^{2-}$, $^{36}Cl^-$, and ^{14}C-oxalate were measured from linear fits to data from the last three time points sampled within each experimental period. For each experiment, water-injected or uninjected oocytes from the same frog were subjected to parallel measurements with cRNA-injected oocytes. Most experimental conditions were tested in oocytes from at least two frogs. Extracellular concentration response curves were fit by a Michaelis-Menten-type equation with

baseline offset, using Sigmaplot 8.0:

$$k_{eff} = k_o + \frac{k_{max} \times [anion]_o}{(K_{1/2} + [anion]_o)}$$

where k_{eff} is the measured $^{36}Cl^-$ efflux rate constant (in min^{-1}), $[anion]_o$ is the concentration of introduced bath substrate anion (in mM), k_o is the $^{36}Cl^-$ efflux rate constant in the absence of extracellular substrate anion, k_{max} is the maximum value of $^{36}Cl^-$ efflux rate constant, and $K_{1/2}$ is the concentration of tested extracellular anion at half-maximal value of k_{max}.

Two-electrode voltage clamp measurements

Microelectrodes from borosilicate glass made with a Sutter P-87 puller were filled with 3 M KCl and had resistances of 2-3 MΩ. Oocytes previously injected with water or with 10 ng of the indicated cRNA were placed in a 1 ml chamber (model RC-11, Warner Instruments, Hamden CT) on the stage of a dissecting microscope and impaled with microelectrodes under direct view. Steady-state currents achieved within 2-5 min following bath change or drug addition were measured with a Geneclamp 500 amplifier (Axon Instruments, Burlingame, CA) interfaced to a Dell computer with a Digidata 1322A digitizer (Axon). Standard recording bath solution was ND-96 (see above). In anion substitution experiments, NaCl was replaced with sodium cyclamate.

Data acquisition and analysis utilized pCLAMP 8.0 software (Axon). The voltage pulse protocol generated with the Clampex subroutine consisted of 20 mV steps between -100 mV and +40 mV, with durations of 738 msec separated by 30 msec at the holding potential of -30 mV. Bath resistance was minimized by the use of agar bridges filled with 3 M KCl, and a virtual ground circuit clamped bath potential to zero during voltage clamp experiments.

Confocal immunofluorescence microscopy

Two or three days after injection with H_20 or with cRNA encoding hSLC26A2, groups of 10-12 oocytes were similarly fixed with 3% PFA and washed with PBS-azide. Oocytes were then placed in PBS containing 1% SDS to permeabilize the surface membranes and unmask epitope. Fixed, permeabilized oocytes were blocked in PBS with 1% bovine serum albumin (PBS-BSA) containing 0.05% saponin for 1 hr at 4°C, then washed three times with PBS-BSA. Oocytes were incubated overnight at 4°C with mouse monoclonal anti-hSLC26A2 antibody IgG2 [24] at 1:400 dilution in PBS-BSA, then washed 3 times in cold PBS-BSA. Antibody-labeled oocytes were then incubated 2 hr at 4°C with Cy3-conjugated secondary goat anti-mouse Ig (Jackson Immunochemicals, diluted 1:500), again thoroughly washed in PBS-BSA, and stored at 4°C until imaging.

Cy3-labeled oocytes were aligned in uniform orientation along a plexiglass groove (gift of P. Grigg, Univ. Mass. Med. Ctr) and sequentially imaged through the 10x objective of a Zeiss LSM510 laser scanning confocal microscope using the 543 nm laser line at 512 x 512 resolution at uniform settings of 80% laser intensity, pinhole 54 (1.0 Airy units), detector gain 650, amplifier gain 1, zero amplifier offset.

Polypeptide abundance at or near each oocyte surface was estimated by quantitation of specific fluorescence intensity (FI) at the circumference of one quadrant of an equatorial focal plane (Image J v. 1.38, National Institutes of Health). Mean background-corrected FI for quadrants of oocytes previously injected with water was subtracted from the background-corrected FI for quadrants of individual cRNA-injected oocytes to yield intensity values for surface-associated specific FI for each oocyte.

Statistics

Data are reported as mean ± SE. Comparisons of two flux data sets was by Student's paired or unpaired two-tailed T tests (Microsoft Excel); multiple flux data were compared by one-way ANOVA with Bonferroni test for post-hoc analysis (SigmaPlot 8.0). Two-electrode voltage clamp currents of control and pendrin-expressing oocytes were compared by unpaired Student's t-test. Currents of pendrin-expressing oocytes in sequential chloride and cyclamate baths were compared by paired Student's t-test. Image intensity data for multiple samples were compared by ANOVA with Bonferroni post-hoc analysis. $P < 0.05$ was interpreted as significant.

Results

Pendrin-mediated chloride/formate exchange is bidirectional

Recombinant pendrin has been shown to transport formate, chloride, iodide, and/or HCO_3^- in *Xenopus* oocytes [23, 35], HEK-293 cells [36-38], HeLa cells [39], and polarized epithelial cells [9]. Fig. 1 shows that pendrin mediated bidirectional Cl^-/formate exchange, with full time courses of ^{14}C-formate efflux stimulated by bath chloride (A,B) and of $^{36}Cl^-$ efflux stimulated by bath formate (C,D). Both transport modes were acutely insensitive to 500 μM DIDS. These results agree with the report of Scott et al [35] that pendrin-mediated $^{36}Cl^-$ uptake was blocked by cis-formate, and that ^{14}C-formate uptake was blocked by cis-chloride. The results also extend their demonstration that single time point measurements of $^{36}Cl^-$ efflux were increased by extracellular formate, and that extracellular chloride increased formate efflux [34].

Extracellular anion selectivity and affinity of pendrin

Extracellular $K_{1/2}$ values for pendrin-mediated anion transport in *Xenopus* oocytes were first reported for 60 min influx of extracellular $^{36}Cl^-$ (2.5 mM) and ^{14}C-formate (0.58 mM) as data not shown [35]. For pendrin-mediated Cl^-/OH^- exchange in HEK-293 cells, $K_{1/2}$ for extracellular chloride was measured as 1.4 mM [40]. Shcheynikov et al. [23] used ion-selective micro-electrodes in *Xenopus* oocytes to demonstrate $K_{1/2}$ for extracellular iodide in the absence (2.7 mM) and presence of 50 mM chloride (25.7

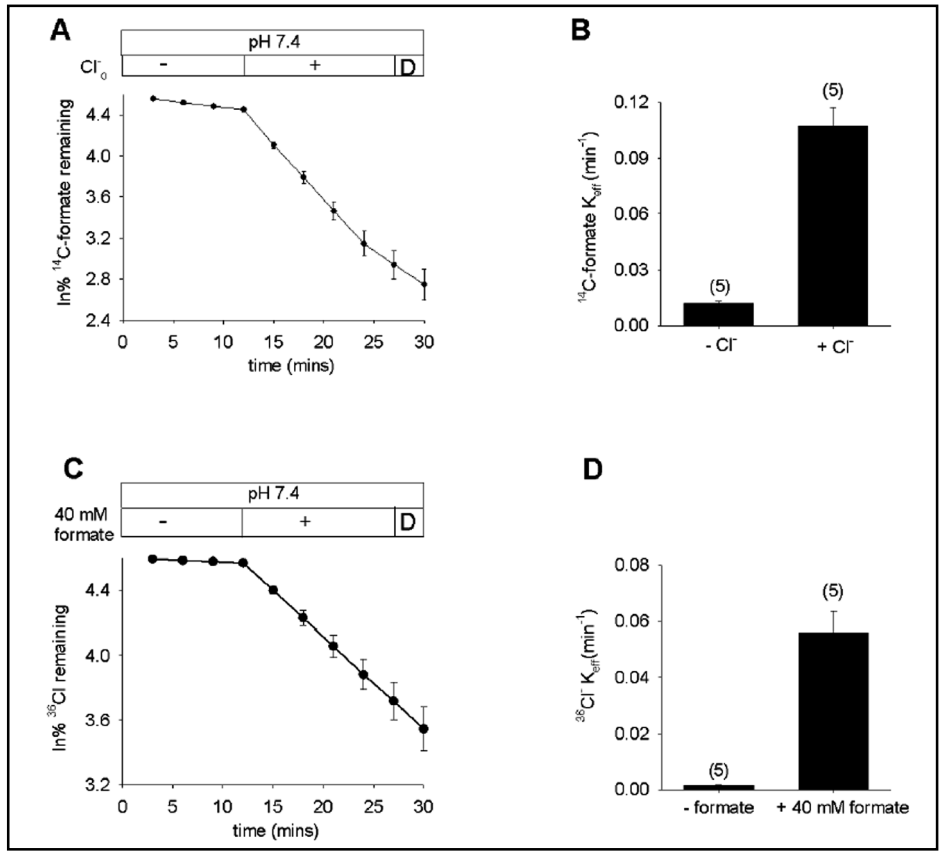

Fig. 1. Pendrin mediates bidirectional formate/Cl^- exchange. A. ^{14}C-formate efflux from pendrin-expressing oocytes exposed sequentially to baths lacking (-) and containing Cl^- (+) followed by a brief exposure to DIDS (D; n=5). B. Mean efflux rate constants for $^{14}C\text{-formate}_{(i)}/Cl^-_{(o)}$ exchange. C. $^{36}Cl^-$ efflux from pendrin-expressing oocytes exposed sequentially to baths lacking (-) and containing 40 mM formate (+), followed by a brief exposure to DIDS (D, n=5). D. Mean efflux rate constants for $^{36}Cl^-_{(i)}/\text{formate}_{(o)}$ exchange.

mM). In iodide-loaded oocytes, the $K_{1/2}$ for extracellular chloride was 14.1 mM.

We have compared $K_{1/2}$ values for extracellular chloride, iodide, bromide, fluoride, and nitrate by measuring $^{36}Cl^-$ efflux from individual oocytes while varying the extracellular [anion]. $K_{1/2}$ for extracellular chloride ($^{36}Cl^-_{(i)}/Cl^-_o$ exchange) was 1.85 mM (n=15, data not shown). Fig 2A shows that $K_{1/2}$ for extracellular iodide ($^{36}Cl^-_{(i)}/I^-_{(o)}$ exchange) was 1.76 mM (n=15). Fig. 2B shows that $K_{1/2}$ for extracellular bromide ($^{36}Cl^-_{(i)}/Br^-_{(o)}$ exchange) was 0.88 mM (n=6).

Extracellular fluoride did not accelerate $^{36}Cl^-$ efflux from oocytes previously injected with 1 ng (n=6) or 10 ng pendrin cRNA (n=6), indicating that $^{36}Cl^-_{(i)}/F^-_{(o)}$ exchange rates were below the level of detection.

Pedemonte et al. showed that apical efflux of nominal intracellular thiocyanate from monolayers of FRTL rat thyroid epithelial cells or primary human bronchial epithelial cells mediating transepithelial secretory thiocyanate transport exhibited respective $K_{1/2}$ values for apical Cl^- of 3.4 and 2.6 mM. They attributed this transport to endogenous pendrin-mediated $Cl^-_{(o)}/SCN^-_{(i)}$ exchange [19]. Pendrin-expressing *Xenopus* oocytes exhibited a $K_{1/2}$ for extracellular SCN^- of 0.13 mM, but V_{max} was 30-40% of that for halides. Bath [SCN^-] exceeding 1 mM

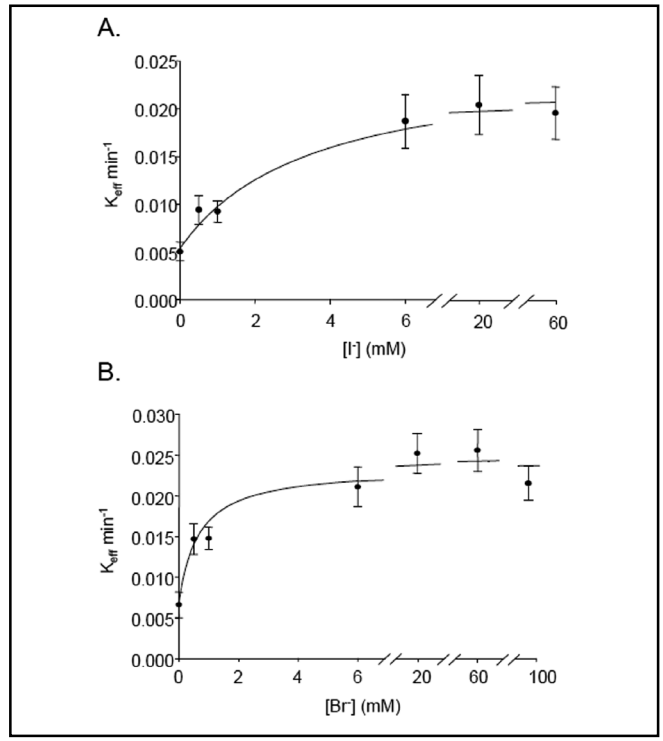

Fig. 2. Extracellular halide $K_{1/2}$ for pendrin-mediated $^{36}Cl^-$ efflux. A. Bath [I^-]-dependence of rate constants for $^{36}Cl^-$ efflux from pendrin-expressing oocytes (n=15). B. Bath [Br^-]-dependence of rate constants for $^{36}Cl^-$ efflux from pendrin-expressing oocytes (n=6).

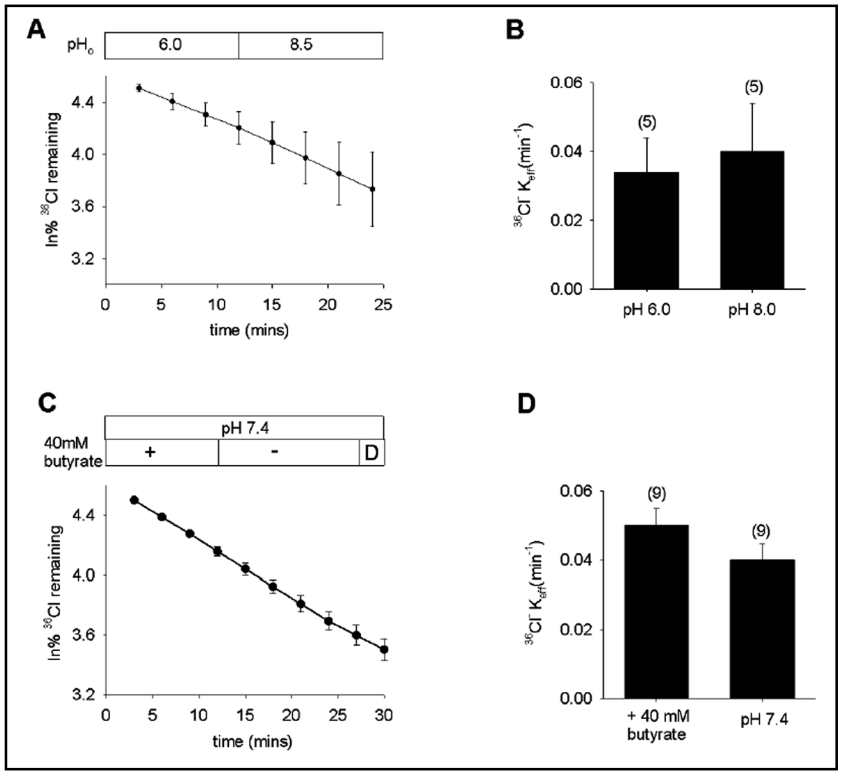

Fig. 3. Pendrin-mediated Cl^-/Cl^- exchange is pH-insensitive in oocytes. A. $^{36}Cl^-$ efflux from 5 pendrin-expressing oocytes subjected to sequential Cl^- baths at pH_o 6.0 and 8.5. B. Mean efflux rate constants for $^{36}Cl^-_{(i)}/Cl^-_{(o)}$ exchange at pH_o 6.0 and 8.5 (n=5). C. $^{36}Cl^-$ efflux from 9 pendrin-expressing oocytes into an initial bath containing 56 mM NaCl and 40 mM Na butyrate, followed by butyrate substitution with 40 mM Na gluconate, and then by a brief exposure to DIDS (D). D. Mean efflux rate constants for $^{36}Cl^-_{(i)}/Cl^-_{(o)}$ exchange in the presence and absence (pH 7.4) of 40 mM butyrate (n=9).

led to robust $^{36}Cl^-$ efflux from both water-injected and pendrin-expressing oocytes (data not shown).

Pendrin-mediated Cl^-/Cl^- exchange in Xenopus oocytes is pH-insensitive

In the lumenal membrane of non-A intercalated cells in the CCD, pendrin is exposed to a range of extracellular pH values (pH_o). However, the rate of pendrin-mediated $^{36}Cl^-_{(i)}/Cl^-_{(o)}$ exchange in oocytes was insensitive to pH_o changes between 6.0 and 8.5 (Fig. 3A,B). Moreover, variation in intracellular pH (pH_i) over 0.5 pH units by bath removal of pre-equilibrated 40 mM butyrate similarly failed to alter the rate of $^{36}Cl^-_{(i)}/Cl^-_{(o)}$ exchange (Fig. 3C,D). Exposure of pendrin-expressing oocytes to 20 mM NH_4Cl, which acidifies oocyte pH_i to values of ~6.9 [34], similarly failed to alter the rate of $^{36}Cl^-_{(i)}/Cl^-_{(o)}$ exchange (n=6, not shown). In contrast, pendrin-mediated Cl^-/OH^- exchange in HEK-293 cells and opossum kidney proximal tubule (OKP) cells was reported to be activated by the same degree of acidic pH_o as well as by a more acidic pH_i [40]. Both regulations were proposed to reflect allosteric effects of pH rather than changes in substrate anion gradient.

Pendrin-mediated Cl^-/Cl^- exchange is not electrogenic

Figure 4 shows that, although pendrin expression was associated with a small but statistically insignificant

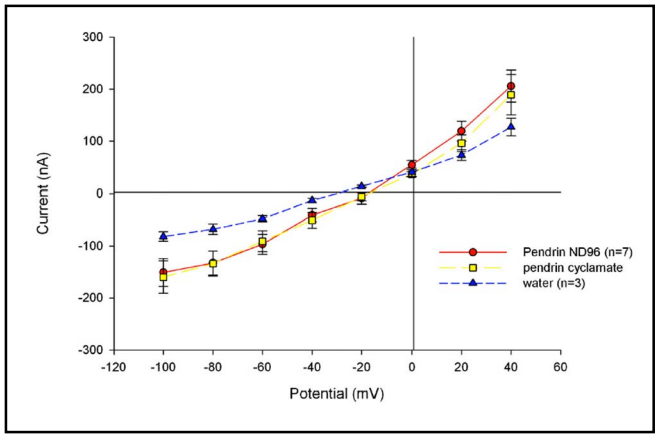

Fig. 4. Pendrin-mediated Cl^-/Cl^- exchange is not detectably electrogenic. Current-voltage (I-V) curve of seven voltage-clamped, pendrin-expressing oocytes exposed first to ND-96 (filled circles) and then to 96 mM sodium cyclamate (squares). Three oocytes previously injected with water (triangles) are shown for comparison.

increase in resting oocyte current as measured in chloride bath (p=0.15), bath chloride substitution with cyclamate did not generate detectably increased current by two-electrode voltage clamp (p=0.29). These data are consistent with the 1:1 stoichiometry of pendrin-mediated Cl^-/HCO_3^- exchange and voltage-independent Cl^-/I^- exchange demonstrated by ion-selective microelectrodes [23] and suggested by halide fluorimetry [41]. The data

Candidate Inhibitor	n	Concentration (mM)	Mean $^{36}Cl^-$ uptake (nmol h^{-1} ± SE)	P-Value	Inhibition (%)
Oocyte background (water-injected)	29		0.17 ± 0.05		
Without drug	24		15.6 ± 1.37		
DIDS, 20°C	14	0.5	18.70 ± 5.49	ns	(0)
DIDS, 37°C	8	0.5	14.72 ± 10.16	ns	(6)
DIDS, 20°C, chloride-free	15	0.5	14.75 ± 6.81	ns	(5)
DIDS, 37°C, chloride-free	8	0.5	19.65 ± 14.53	ns	(0)
Tenidap	19	0.1	7.92 ± 1.23	<0.001	**49**
Niflumic acid	10	0.1	8.41 ± 1.58	0.020	**46**
NS 3623	8	0.1	10.1 ± 2.37	ns	(35)
Hydrochlorothiazide	10	1	10.6 ± 1.01	ns	(32)
Flufenamic acid	10	0.1	11.9 ± 2.05	ns	(24)
PMA	10	0.01	12.1 ± 2.18	ns	(23)
α-Cyano-3-hydroxy-cinnamic acid	10	1	13.5 ± 1.61	ns	(13)
6-Ethoxy-2-Benzothiazolesulfenamide	10	0.1	14.1 ± 1.76	ns	(10)
Wortmannin	10	0.1	15.7 ± 2.32	ns	(0)
UK 5099	9	1	16.9 ± 1.65	ns	(0)
4-Hydroxy-cinnamic acid	6	1	19.6 ± 3.35	ns	(0)
Levamisole	9	1	21.0 ± 2.08	ns	(0)
Trans-cinnamic acid	9	1	22.1 ± 1.55	ns	(0)

Table 1. Tests of candidate inhibitors of pendrin-mediated $^{36}Cl^-$ influx. % inhibition is presented in bold if statistically significant ($p<0.05$, one-way ANOVA), and in gray in parentheses if $p>0.05$.

taken together document electroneutrality of pendrin-mediated monovalent anion exchange.

Pendrin inhibitors are few and of low potency

Mouse pendrin and Slc4a8 function as a NaCl cotransporter (NCC)-independent, thiazide-sensitive NaCl reabsorption system of the CCD [11], suggesting pendrin as a target for novel diuretic or cardiotonic drugs. However, hydrochlorothiazide does not inhibit pendrin at concentrations consistent with this NCC-independent effect [11]. Indeed, strong inhibitors of pendrin have not been identified. Although pendrin is commonly described as DIDS-insensitive, pendrin-mediated Cl^-/OH^- exchange activity was recently reported as sensitive to 500 μM DIDS [40], echoing an earlier report of DIDS-sensitivity [37]. Indeed, Emmons reported that lumenal membrane Cl^-/HCO_3^- exchange in perfused rabbit CCD was insensitive to 200 μM DIDS in the presence of Cl^-, but inhibited 67% after lumenal DIDS pre-incubation in Cl^--free medium [42]. As shown in Table 1, neither acute room temperature exposure to 500 μM DIDS nor 30 min DIDS pre-incubation of pendrin-expressing oocytes in the absence of Cl^- led to measurable pendrin inhibition. Elevation of DIDS preincubation temperature to 37°C did not unmask inhibition of pendrin by DIDS. Tests of other drugs in the presence of Cl^- revealed only 100 μM niflumate and 100 μM tenidap as modest inhibitors of pendrin. These two drugs exhibit greater potency as inhibitors of SLC26A3, a pendrin paralog of minimal DIDS-sensitivity [25].

Amino acid residues tolerated at pendrin residue E303

Pendrin E303Q is a missense mutation found in compound heterozygosity with loss-of-function pendrin mutation H723R. Pendrin E303Q exhibits loss of anion transport function for Cl^-, I^-, and HCO_3^-, despite the mutant protein's accumulation at the *Xenopus* oocyte surface at wildtype levels [4]. E303 of pendrin is modeled at the N-terminal cytoplasmic end of putative transmembrane span 7, based on topographical fusion protein studies of bacterial SulP bicarbonate transporter BicA and plant sulfate transporter SHST1 [43], although earlier models based solely on hydropathy profiling predicted a more exofacial location. To explore the range of amino acid side chains tolerated at pendrin residue 303, we substituted residues of distinct charge and size. As shown in Fig. 5A for oocytes injected with 1 ng cRNA, all tested substitutions yielded mutants with activity lower than that

of wildtype pendrin. However, only substitutions K and S were as severely affected as disease mutant E303Q. Since mutant overexpression allows functional expression of some mutants, we tested the effects of injection of 10 ng mutant cRNA (Fig. 5B). In this condition, E303 substitutions with D, C, A, S, and N exhibited activity near or exceeding that exhibited by oocytes expressing 1 ng wildtype pendrin. However, E303Q remained hypofunctional, and E303K completely nonfunctional. As the charge reversal mutation E303K produced the most complete loss-of-function, we tested the effect of chemical charge modification at E303C. Oocytes expressing 10 ng cRNA encoding pendrin E303C were treated with extracellular MTSES (to derivatize the Cys sulfhydryl group at position 303 with a negative charge), MTSET (to confer a positive charge), or MTSEA (to confer a pH-sensitive positive charge). None of the MTS reagents reduced $^{36}Cl^-$ influx by oocytes expressing pendrin E303C. Thus, E303 of pendrin was inaccessible to all MTS reagents, consistent with a location within the bilayer or forming part of a cytoplasmic surface vestibule [43]. Alternatively, introduction of positive charge at E303 does not suffice to replicate the functional deficit of mutant E303K, and side chain steric factors may also be important.

E-to-Q mutations in other SLC26 polypeptides at positions analogous to pendrin E303

The conservation of pendrin E303 among nearly all SLC26 polypeptides [4] prompted a test of the hypothesis that the functional characteristics of pendrin mutant E303Q are also conserved in the corresponding mutants of other SLC26 anion exchangers. Human SLC26A2 mediates sulfate uptake into *Xenopus* oocytes [24], but SLC26A2 mutant E336Q exhibited nearly complete loss-of-function whether influx was measured in 1 mM or 20 mM sulfate, or after injection of 40-fold excess mutant cRNA (Fig. 6A). Despite its loss-of-transport function, SLC26A2 E336Q was expressed at the oocyte surface at wild-type abundance (Fig. 6B), resembling pendrin E303Q in both respects. Human SLC26A3-mediated $^{36}Cl^-$ uptake was completely abolished in SLC26A3 mutant E293Q (Fig. 6C). The mutation also abolished SLC26A3-mediated $^{36}Cl^-_{(i)}/Cl^-_{(o)}$ exchange (Fig. 6D).

The $^{14}C\text{-oxalate}_{(i)}/Cl^-_{(o)}$ exchange activity of human SLC26A6 [26, 44] was nearly abolished by the homologous SLC26A6 mutation E298Q (Fig. 7A,B). SLC26A6-mediated uptakes of ^{14}C-oxalate (Fig. 7C) and of $^{36}Cl^-$ (Fig. 7D) were similarly impaired by the E298Q mutation. Thus, E-to-Q missense substitutions in SLC26A2, -A3, and -A6 in positions homologous to E303 of pendrin produce similar loss-of-function phenotypes.

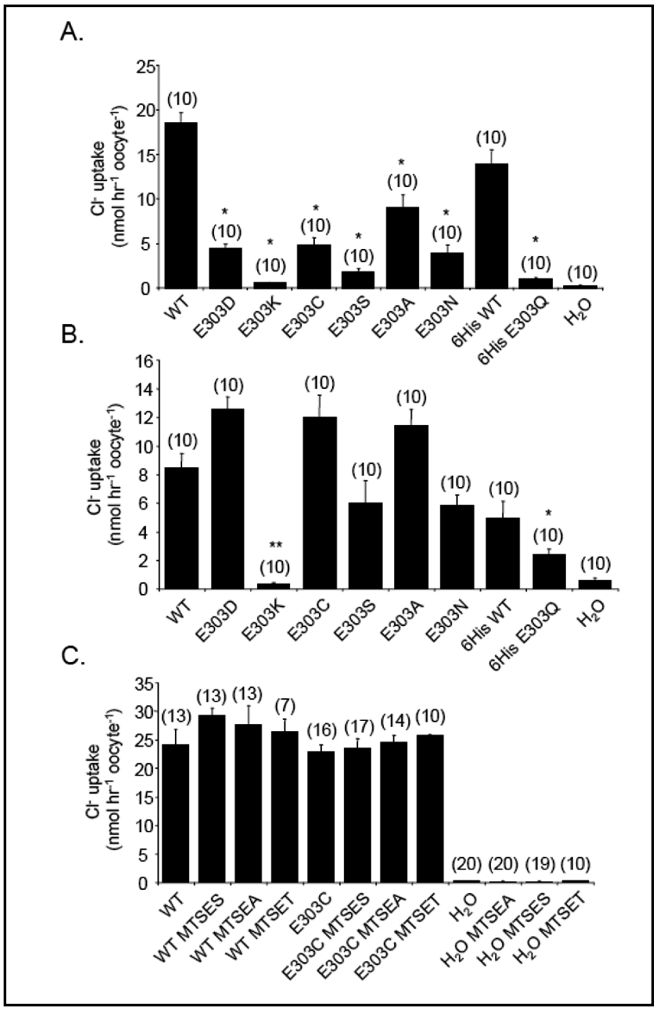

Fig. 5. Pendrin E303 missense substitutions show a range of functional impairment. A. $^{36}Cl^-$ influx into oocytes previously injected with water or with 1 ng cRNA encoding wildtype (WT) pendrin, WT pendrin-6His, pendrin E303Q-6His, or the indicated E303 missense mutant pendrin polypeptides without a C-terminal 6His tag. *, $p<0.001$ WT vs all E303 mutants; $p<0.001$ WT-6His vs. E303Q-6His. B. $^{36}Cl^-$ influx into oocytes previously injected with water, with 1 ng cRNA encoding WT pendrin or WT pendrin-6His, or with 10 ng cRNA encoding the indicated E303 missense pendrin mutant polypeptides. *, $p<0.05$ E303Q-6His vs WT-6His; **, $p<0.001$ vs. WT; C. $^{36}Cl^-$ influx into oocytes previously injected with water or with 10 ng cRNA encoding wildtype 6His (WT) or E303C pendrin in the absence or presence of 10 mM MTSES, 5 mM MTSEA, or 1 mM MTSET. Oocytes were preincubated with MTS reagents 15 min prior to initiation of the influx period.

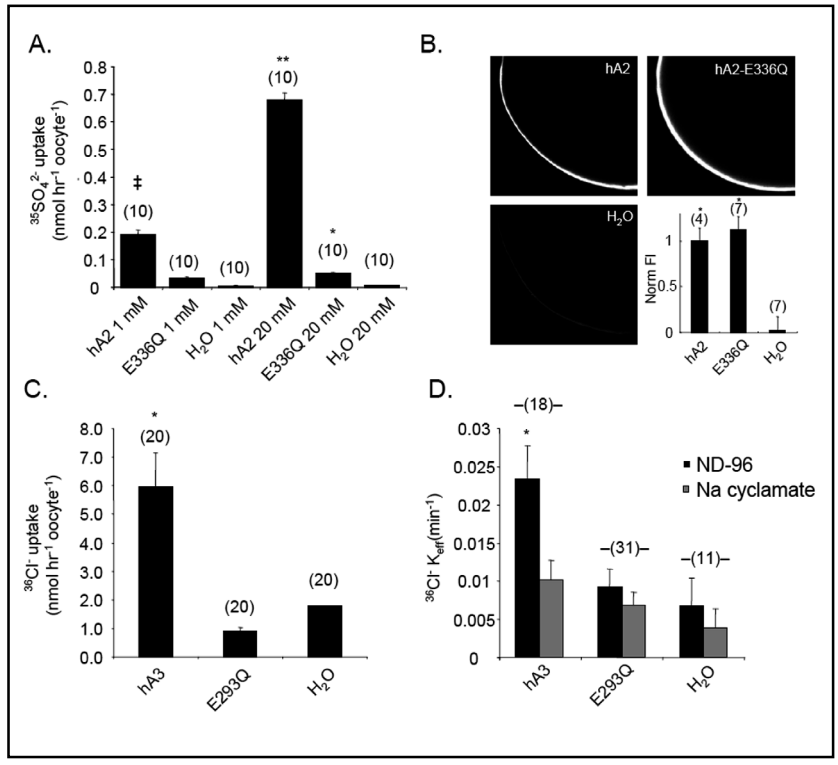

Fig. 6. SLC26A2 E336Q is a loss-of-function mutation with wildtype surface expression, and SLC26A3 E293Q exhibits similar loss of function. A. $^{35}SO_4^{2-}$ influx from cyclamate baths containing 1 mM or 20 mM sulfate into oocytes previously injected with water or with 0.5 ng cRNA encoding wildtype SLC26A2 (hA2) or 20 ng cRNA encoding SLC26A2 mutant E336Q (n=10). ‡, p<0.05 vs E336Q, p< 0.005 vs. water in 1 mM sulfate; **, p<0.001 vs. E336Q; *, p<0.001 vs. water in 20 mM sulfate. B. Confocal immunofluorescence images of representative median intensity showing oocytes previously injected with water or with 10 ng cRNA encoding SLC26A2 (hA2) or its mutant E336Q. Lower right, average fluorescence intensities for (n) oocytes. P<0.005 vs water. C. $^{36}Cl^-$ influx into (n) oocytes previously injected with water or with 10 ng cRNA encoding SLC26A3 (hA3) or its mutant E293Q (20 ng). *, p < 0.005 vs E293Q or water. D. $^{36}Cl^-$ efflux rate constants into ND-96 bath for (n) oocytes previously injected with water or with 10 ng cRNA encoding SLC26A3 (hA3) or 20 ng encoding SLC26A3 mutant E293Q. *, p < 0.05 vs E293Q, 0.005 vs. water.

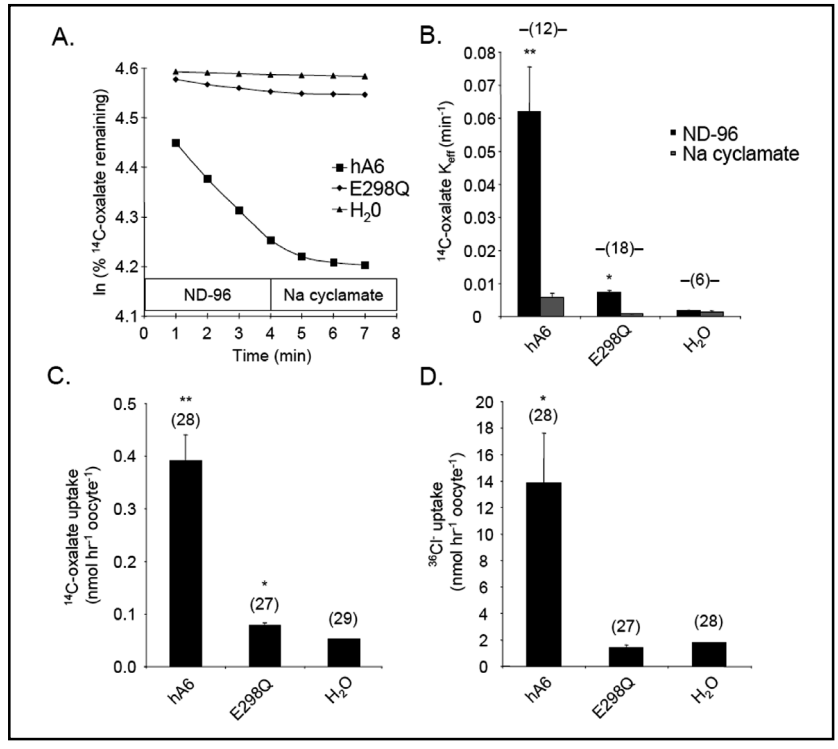

Fig. 7. SLC26A6 E298Q is a loss-of-function mutation. A. ^{14}C-oxalate efflux traces into sequential baths of ND-96 and sodium cyclamate, from individual representative oocytes previously injected with water or with cRNA encoding wildtype SLC26A6 (hA6) or its mutant SLC26A6 E298Q. B. Mean ^{14}C-oxalate efflux rate constants measured from (n) oocytes previously injected with water or with cRNA encoding SLC26A6 (hA6, 10 ng) or mutant E298Q (20 ng). **, p<0.01 vs, E298Q, 0.001 vs. water; *,p <0.01 vs. water. C. ^{14}C-oxalate uptake into (n) oocytes previously injected with water or with cRNA encoding SLC26A6 (hA6, 10 ng) or its mutant E298Q (20 ng). **, p<0.001 vs. E298Q or water; *, p<0.05 vs. water. D. Mean $^{36}Cl^-$ influx into (n) oocytes previously injected with water or with cRNA encoding SLC26A6 (hA6, 10 ng) or its mutant E298Q (20 ng). *, p<0.05 vs. E298Q or water.

Pendrin differs from SLC26A2, SLC26A3, and SLC26A6 in its lack of inhibition by protein kinase Cδ

Mouse Slc26a6/CFEX was shown by Hassan et al. to be inhibited by the protein kinase C (PKC) agonist phorbol 12-myristate 13-acetate (PMA), whereas pendrin was insensitive to PMA. This PMA inhibition of Slc26a6 was not reversed by inhibitors of classical PKC isoforms, but was partially reversed by rottlerin, a drug used as an inhibitor of protein kinase Cδ, (PKCδ) [45]. However, rottlerin does not inhibit purified recombinant PKCδ [46] but may indirectly inhibit a range of

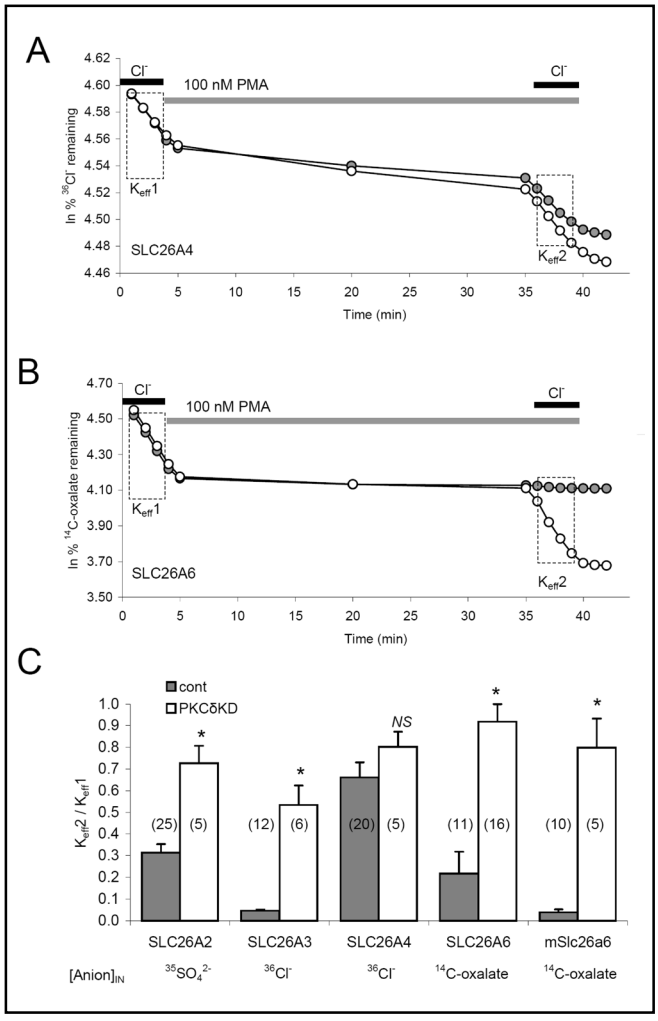

Fig. 8. Protein kinase Cδ inhibits anion exchange mediated by hSLC26A2, hSLC26A3, hSLC26A6, or mSlc26a6, but not pendrin hSLC26A4. A. $^{36}Cl^-$ efflux traces from representative, individual oocytes previously injected with 1 ng hSLC26A4 cRNA without (filled circles) or with 50 ng hPKCδ-kinase-dead (hPKCδ-KD) cRNA (open circles). Oocytes were exposed sequentially to baths containing ND-96, Cl^--free cyclamate containing 100 nM PMA, ND-96 in the continued presence of PMA, then Cl^--free cyclamate. B. ^{14}C-oxalate efflux traces from representative individual oocytes previously injected with 5 ng hSLC26A6 cRNA without (filled circles) or with 50 ng hPKCδ-KD cRNA (open circles), and exposed to the same sequence of bath solutions as in panel A. C. Mean ratios of efflux rate constants before ($K_{eff}1$) and after ($K_{eff}2$) PMA exposure comparing (n) oocytes expressing anion exchanger alone (gray bars) or together with hPKCδ-KD (white bars). *, $p < 0.0005$ vs absence of hPKCδ-KD.

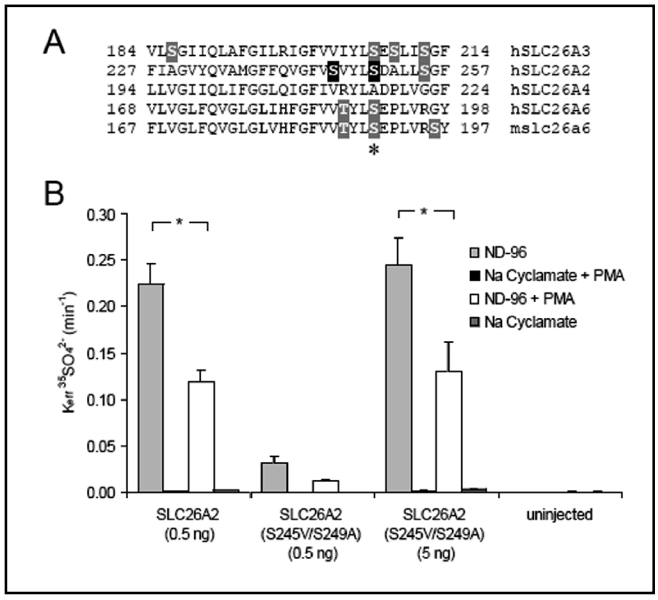

Fig. 9. Mutation of SLC26A2 Ser residues conserved among PMA-sensitive SLC26 gene products but absent from pendrin did not alter PMA inhibition of SLC26A2. A. Alignments of SLC26 anion exchangers tested in Fig. 7 showed one region (pictured) in which Ser and Thr residues (highlighted) were conserved in PMA-sensitive transporters but not in PMA-insensitive SLC26A4. hSLC26A2 S245 and S249 (highlighted in black) were selected for mutagenesis. B. Mean $^{35}SO_4^{2-}$ efflux rate constants from (n) oocytes studied as in panel B of Fig. 8. *, $p < 0.00005$, pre- vs. post-PMA.

kinases by uncoupling mitochondrial respiration to lower cellular [ATP] [47, 48]. This and other pharmacological actions, such as activation of the BKCa channel [49], left unclear the mechanism by which rottlerin antagonized inhibition of Slc26a6 by PMA [50].

We re-examined the role of PKCδ as a selective regulator of SLC26 transporters by assessing the effect of PMA on SLC26 transporters coexpressed without or with the kinase-dead K376A variant of mouse PKCδ (PKCδ-KD; [29]). As shown in Fig. 8A and summarized in Fig. 8C, PMA exposure inhibited pendrin-mediated $^{36}Cl^-_{(i)}/Cl^-_{(o)}$ exchange by ~30% whether with or without coexpressed PKCδ-KD. In contrast, PMA treatment of oocytes expressing human SLC26A6 inhibited SLC26A6-mediated ^{14}C-oxalate/$Cl^-_{(o)}$ exchange by at least 80%, but coexpression with PKCδ-KD largely prevented the inhibitory effect of PMA treatment (Fig. 8B, 8C). PMA exposure also inhibited mouse Slc26a6-mediated ^{14}C-oxalate/$Cl^-_{(o)}$ exchange and human SLC26A3-mediated $^{36}Cl^-_{(i)}/Cl^-_{(o)}$ exchange by 95%, and human SLC26A2-mediated $^{35}SO_4^{2-}{}_{(i)}/Cl^-_{(o)}$ exchange by 70%. In each case, co-expression of PKCδ-KD largely abrogated the inhibition produced by 30 min exposure to PMA. Thus, PMA dramatically reduces anion exchange activity of

SLC26A6, SLC26A3, and SLC26A2, and this effect is indeed largely through activation of PKCδ as originally proposed for mSlc26a6-mediated oxalate influx [45]. In contrast, the modest inhibition of pendrin by PMA was not mediated through PKCδ.

Pendrin insensitivity to PKCδ is not explained by the absence of two candidate Ser residues conserved in PMA-responsive SLC26 anion exchangers

Since activated PKCδ strongly inhibits SLC26A6, A3, and A2, but does not inhibit pendrin, we searched for Ser and Thr residues conserved in SLC26A6, -A3, and -A2, but not in SLC26A4. One such Ser residue (Fig. 9A, asterisk) is present in all the PKCδ-sensitive transporters in the second intracellular loop between putative transmembrane spans 4 and 5 (per topography of [43]), but not in pendrin. A Thr residue three positions away in SLC26A6 and another Ser residue four residues away in SLC26A2 also align with non-phosphorylatable residues in pendrin (Fig. 9A). We tested these residues as candidate phosphorylation targets for PKCδ-mediated inhibition of SLC26A2. Residues S249 and S245 of SLC26A2 were mutated to the corresponding pendrin residues, and the resulting SLC26A2 double mutant was examined for loss of PMA-sensitivity of sulfate uptake, and acquisition of the PMA-resistant phenotype of pendrin. As shown in Fig. 9B, SLC26A2 double mutant S245V/S249A was inhibited by PMA to the same degree as was wildtype SLC26A2. Although the double mutant exhibited reduced functional expression levels, the preserved inhibitory effect of PMA was evident in oocytes injected with either 0.5 or 5 ng cRNA (associated with function equivalent to that of 0.5 ng wildtype SLC26A2). Thus, inhibition by PMA of SLC26A2 does not require phosphorylation of the two studied serine residues of the second intracellular loop of the transmembrane domain that are not present in the corresponding positions of pendrin. We hypothesize that the corresponding phosphorylatable residues in SLC26A3 (S206) and SLC26A6 (S190) are also not required for inhibition by PMA-activated PKCδ.

Discussion

Anion selectivity and affinity

Pendrin and many SLC26 paralogs transport multiple anions in varied physiological and *in vitro* contexts. It is then of interest to compare pendrin's rank orders of anion transport rate and cis-competition, and to compare these rank orders with those of other SLC26 and SLC4 anion exchangers and conductances. The interaction between a mobile anion substrate and its transporter binding site (both modeled as hard spheres) was represented by Eisenman (with elaboration by Wright, Diamond, and others) as a balance between the enthalpic energy of substrate anion dehydration and the electrostatic interaction between dehydrated anion and its transporter binding site. This balance was described by the concept of electrostatic field strength of the binding site [51]. For high field-strength sites (Eisenman sequence 5), the enthalpic energy of anion dehydration exceeds that of the ion's electrostatic interaction with the idealized binding site, whereas for low field-strength sites (Eisenman sequence 1), the electrostatic interaction of ion with binding site exceeds that of anion dehydration. Although this formulation did not consider entropic costs of ion binding, binding site dynamics within the protein influencing kinetics of anion desolvation and binding, or possible roles of water molecules within or adjacent to the binding site [52, 53], the resulting predicted anion rank orders 1 through 5 can account for most cases of biological anion transport.

Pendrin expressed in *Xenopus* oocytes displays an extracellular $K_{1/2}$ halide rank order of $Br^- > I^- = Cl^- > F^-$ (Eisenman sequence 2 or 3), and a V_{max} rank order of $Cl^- > Br^- = I^-$. These rank orders differ from that for cis-inhibition of $^{36}Cl^-$ influx by 5 mM extracellular anion: $I^- > NO_3^-$ = formate > Br- > Cl^- (Eisenman sequence 1) [35]. Endogenous pendrin activity in isolated perfused rabbit CCD exhibited a lumenal halide V_{max} rank order of $Cl^- = Br^- > I^- > F^-$ (Eisenman sequence 4) for lumenal anion/HCO_3^- exchange [54, 55]. Thus the V_{max} halide rank order of human pendrin in *Xenopus* oocytes parallels that of putative rabbit CCD pendrin. However, distinct halide rank orders apply for pendrin V_{max}, $K_{1/2}$, and external cis-inhibition, likely reflecting different electric field strengths in the vicinity of pendrin amino acid residues governing ion translocation, anion binding and release, and competitor anion binding. Rank orders of cis-inhibition displayed lower field strength patterns, suggesting involvement of peripheral binding sites.

Mouse Slc26a6-mediated oocyte $^{36}Cl^-_i/Cl^-_o$ exchange revealed a V_{max} rank order of $Cl^- > Br^- = NO_3^- > HCO_3^-$ (Eisenman sequence 5 or 4) [26], and human SLC4A2/AE2-mediated $^{36}Cl^-_i/Cl^-_o$ exchange revealed a V_{max} rank order of $Cl^- = NO_3^- > Br^-$ > isethionate = gluconate > I^- (Eisenman sequence 4 or 5; [56]. SLC4A1/AE1 of the intact human erythrocyte exhibited an a $Cl^-_{(i)}/X^-_{(o)}$ exchange V_{max} rank order (at 23°C) of $Cl^- > Br^- >$

$F^- > I^-$ (Eisenman sequence 5). Thus, anion exchange mechanisms of both SLC4 and SLC26 gene families shared V_{max} rank orders of Eisenman sequence 4 or 5, consistent with high field strength binding sites being rate-limiting for transport. Rank orders of extracellular halide $K_{1/2}$ values have not been reported for other SLC26 anion exchangers.

AE1-mediated Cl^-/Cl^- exchange in intact human erythrocytes displayed halide rank-orders of cis-inhibition and conductive anion permeability of $I^- > Br^- > Cl^-$ (Eisenman sequence 1) [57]. *Xenopus* oocytes expressing human AE1 Δ6-7 (an engineered mutant lacking putative transmembrane spans 6 and 7) exhibited the same halide rank order of anion conductance [58]. The permselectivity rank order of anion channel SLC26A9 ($I^- > Br^- > NO_3^- > Cl^-$; Eisenman sequence 1) differed from its rank order of conductance ($Br^- > Cl^- > I^- > NO_3^-$; Eisenman sequence 3) [59], and both differed from the shared permselectivity and conductance rank orders of anion channel SLC26A7 ($NO_3^- > Cl^- = Br^- = I^-$; Eisenman sequence 4) [60]. Thus, permselectivities associated with recombinant SLC26A9 in oocytes and with native erythrocyte SLC4A1 shared Eisenman sequence 1, suggesting anion binding sites of low field strength rather than the high field strength associated with sites involved in SLC4- and SLC26-mediated anion exchange. However, conductance rank orders differed between the ion channel activities of SLC26A9 and SLC26A7, and permselectivity and conductance rank orders differed for SLC26A9.

Our finding of electroneutral Cl^-/base exchange by pendrin supports a previous report that pendrin-mediated Cl^-/I^- and I^-/HCO_3^- and Cl^-/HCO_3^- exchanges in *Xenopus* oocytes are electroneutral, with stoichiometry of 1:1 [23]. The slightly elevated bath Cl^--independent current observed in pendrin-expressing oocytes might be related to previous reports of pendrin overexpression-associated activation in HEK-293 cells of apparently endogenous cation currents [61] and activation in COS-7 cells of currents of different character [62].

Sensitivity of pendrin activity to pH

Our observation that pendrin-mediated Cl^-/Cl^- exchange in *Xenopus* oocytes was independent of both pH_o and pH_i differed from the reported activation of pendrin-mediated Cl^-/OH^- exchange in HEK-293 cells by both acidic pH_i and by acidic pH_o [40]. This difference may reflect the presence of a pH-sensitive regulatory component that is present or active in HEK-293 cells at 37°C but absent or inactive in *Xenopus* oocytes at room temperature. However, the two data sets differed in other ways, as well. Oocyte $^{36}Cl^-_i/Cl^-_o$ exchange experiments were carried out at nominal steady-state for both intracellular and extracellular substrate, whereas HEK-293 cell Cl^-/OH^- exchange was measured under maximal gradient conditions, initiated by restoration of 120 mM Cl^-_o for assessment of pH_o sensitivity, and by bath Cl^- removal with simultaneous acute pH_o change for determination of pre-equilibrated pH_i sensitivity. Whereas our oocyte study varied pH_i values between ~6.6 and 7.1 at constant pH_o, Azroyan et al. [40] studied a wider range of pH_i values (6.2-7.5) in the setting of acutely elevated pH_o. Their calculation of H^+-equivalent transport rates used an unreported value of intrinsic buffer capacity (β_i) determined from a single alkalinizing pH step of 20 mM NH_4Cl, without evident allowance for the commonly observed pH_i-dependent variation of β_i.

The reported 3-fold activation of pendrin-mediated Cl^-/OH^- exchange across a 100-fold range of extracellular $[OH^-]$, and the 2-fold activation over a 20-fold range of intracellular $[OH^-]$ is consistent with gradients of substrate $[OH^-]$ imposed by the assay. However, pendrin regulation by both pH_i and pH_o was interpreted as allosteric, based on mathematical modeling with the assumption of symmetrical intracellular and extracellular binding affinities for each ion [40]. This assumption disregards the different amino acid side chains surrounding internal and external anion binding sites, and contrasts with evidence for SLC4A1/AE1 indicating divergent apparent binding affinities of internal and external anion binding sites [63]. Tests of pH-dependence of anion rank order have not been reported for $K_{1/2}$, k_{max}, or cis-inhibition of pendrin-mediated anion exchange.

Sensitivity of pendrin activity to inhibitors

The first report of pendrin-mediated $^{36}Cl^-$ uptake into *Xenopus* oocytes from a bath containing 5 mM Cl^- noted 62% inhibition by 1 mM DIDS [64]. Pendrin-mediated Cl^-/HCO_3^- exchange in HEK-293 cells was sensitive to 0.5 mM DIDS in the absence of extracellular Cl^- [37] and in Cl^--free bath containing 15 mM HCO_3^- in the absence of added CO_2 [40]. DIDS sensitivity was also reported for endogenous anion exchange activities ascribed to pendrin. Thus, in isolated perfused rabbit CCD, apical Cl^-/OH^- exchange in the presence of lumenal Cl^- was insensitive to 0.2 mM DIDS, but partially sensitive to 0.1 mM DIDS following 30 min preincubation of drug in the absence of Cl^- [42]. In pendrin-expressing spiral prominence epithelial cells of gerbil cochlea, Cl^-/OH^- exchange (measured in the presence of 15 mM extracellular Cl^-) was abolished by 1 mM DIDS [7].

In contrast, recombinant pendrin-mediated $^{36}Cl^-$ influx into HEK-293 Phoenix cells from a bath containing physiological [Cl^-] was insensitive to 0.5 mM DIDS [36]. DIDS-insensitivity of endogenous pendrin-like activity was corroborated by Cl^- flux studies in FRTL-5 thyroid epithelial cells co-expressing pendrin and an optimized EYFP halide sensor [19], and further corroborated by the DIDS-insensitivity of native human pendrin in Calu-3 airway submucosal gland epithelial cells [65]. Our current results with pendrin-mediated $^{36}Cl_{(i)}/Cl^-_{(o)}$ exchange in Xenopus oocytes indicate insensitivity to 0.5 mM DIDS (Calbiochem) with or without 30 min preincubation in Cl^--free bath, at 20°C or 37°C. The differences in reported DIDS sensitivity of pendrin are not easily explained by differences in expression system or temperature. Preferential DIDS inhibition of pendrin-mediated Cl^-/base exchange vs. Cl^-/Cl^- exchange may reflect the difference between 10-100 nM extracellular [OH^-] and 15-100 mM extracellular [Cl^-]. In addition, commercial DIDS preparations can contain or evolve impurities with distinct pharmacological properties [66] that might contribute to the different pharmacological results.

We evaluated cinnamic acid derivatives because α-cyano-4-hydroxy-cinnamic acid inhibited rabbit CCD lumenal Cl^-/HCO_3^- exchange (nominally pendrin) with an IC_{50} of 2.4 mM [42]. In addition, Simchowitz reported that the human neutrophil Cl^-/HCO_3^- exchanger (of still unknown identity) was inhibited 90% by 40 mM cyano-OH-cinnamate, and much more potently by 400 μM UK-5099 ($K_{1/2}$ was 48 μM in the presence of 148 mM Cl^-, and 2.3 μM in the presence of 2.5 mM (Cl^--free) HCO_3^- [67]. We found that neither drug inhibited pendrin expressed in *Xenopus* oocytes. Pendrin was similarly insensitive to inhibition by CFTR inhibitors GlyH-101 and PPQ-102 at concentrations that substantially inhibited guinea pig Slc26a11 and (in the case of GlyH-101) moderately inhibited guinea pig Slc26a3 and Slc26a6 [68]. A screen of pendrin-expressing EYFP-FRTL-5 cells with a 2000 compound chemical library did not discover any Cl^-/I^- exchange inhibitors other than modest inhibition by niflumate [19] as previously described [61], and confirmed here (Table 1).

An important glutamate residue in putative TM7 of multiple SLC26 anion exchangers

Transmembrane domain glutamate residues have proven to be important contributors to the mechanism of anion transport. A critical glutamate governs coupling of H^+ and SO_4^{2-} with counterport of Cl^- in SLC4A1/AE1 [69, 70]. Two critical glutamates control coupling of Cl^-/H^+ exchange by the *E. coli* Clc-ec1 protein [71]. Modeling of SLC26 transporters on the structure of the *E. coli* Clc-ec1 Cl^-/H^+ exchanger polypeptide, although unrelated in primary sequence, identified two highly conserved glutamate residues with important roles in tight coupling of anion exchange [72].

Pendrin E303Q is unusual as a Pendred Syndrome mutation in its combination of severe loss-of-function with retention of oocyte surface expression [4]. E303 may reside in the middle of putative TM7 [43], a transmembrane span modeled to include several charged residues. Pendrin E303 is conserved among 9 of 10 SLC26 polypeptides, with minimal divergence to Asp in SLC26A7. The corresponding E-to-Q mutations in SLC26A2, SLC26A3, and SLC26A6 produce similar phenotypes of loss-of-transport function and (in the case of SLC26A2) maintenance of wildtype surface expression. These data support the contention that this Glu residue also contributes in important ways to the anion exchange mechanism of these several SLC26 polypeptides. The lack of effect of MTS reagents on functional mutant pendrin E303C suggests side chain inaccessibility under the high bath Cl^- conditions tested. Several E303 mutants were hypofunctional in oocytes, but with the sole exception of E303K, activity of the other mutants was partially or fully rescued by forcing overexpression. This phenotype suggests milder, stochastic folding defects that might be unmasked with longer time or higher temperature.

Pendrin differs from other SLC26 anion exchangers in its insensitivity to inhibition by PKCδ

Hassan et al. demonstrated the powerful inhibition by phorbol ester of mSlc26a6/CFEX but not pendrin expressed in *Xenopus* oocytes. They further showed that inhibitors of classical PKCs were ineffective in countering the effect of PMA. However, attenuation of the PMA effect by 10 μM rottlerin prompted the proposal that the PMA effect reflected activation of PKCδ, and that PKCδ inhibited mSlc26a6 but not pendrin [45].

Since the specificity and efficacy of rottlerins's action on PKCδ has been questioned [46,48], we investigated the role of PKCδ in PMA regulation of SLC26 anion exchangers by assessing the effects of coexpression of kinase-dead PKCδ. We confirmed PMA inhibition of mSlc26a6, and showed that PMA also inhibited hSLC26A6, hSLC26A3, and hSLC26A2. We further showed that PMA only modestly inhibited pendrin-mediated $^{36}Cl^-_{(i)}/Cl^-_{(o)}$ exchange. Coexpression of kinase-

dead PKCδ with SLC26 exchangers led to reduction or abolition of PMA-induced inhibition, with the sole exception of pendrin. These results thus support the proposal of Hassan et al [45], that oocyte treatment with PMA inhibits mSlc26a6 through activation of PKCδ, despite the shortcomings of rottlerin as a diagnostic inhibitor. Our results also extend the hypothesis of Hassan et al. to human SLC26A6, -A3, and -A2.

To evalute the possibility that the lack of PKCδ regulation of pendrin might reflect a lack of direct phosphoryation, we searched for Ser and Thr residues conserved in the PKCδ-sensitive transporters but absent from pendrin. We found one such Ser residue in SLC26A2, but its mutation in tandem with mutation of a nearby Ser to the corresponding hydrophobic residues present in the PKCδ-insensitive pendrin failed to reduce the inhibitory effect of PKCδ on SLC26A2. This result suggests either PKCδ acts through phosphorylation of other target residues, or that PKCδ-mediated inhibition of SLC26 transporters is indirect. Interestingly, in PC C13 thyrocytes in which endogenous pendrin expression was previously induced by TSH and insulin, PKCε activation appears to promote translocation of pendrin from internal stores to the cell surface [73]. PKCδ and PKCε have also been reported to exert opposing actions on cardiac myocyte hypertrophy [74]. Additional components of the SLC26 PKCδ signaling cascade that do not affect pendrin have not yet been reported.

Acknowledgements

This work was supported by NIH grants R01 DK43495 and HL077765 (SLA), by a grant from the US-Israel Binational Science Foundation (SLA and IZ) and by the Harvard Digestive Diseases Center DK34854 (SLA and AKS). FRR was supported by a postdoctoral fellowship from the Robert-Bosch-Stiftung. JFH was supported by NIH T32 postdoctoral fellowship grants DK07094, DK07477, and DK007199.

References

1 Everett LA, Glaser B, Beck JC, Idol JR, Buchs A, Heyman M, Adawi F, Hazani E, Nassir E, Baxevanis AD, Sheffield VC, Green ED: Pendred syndrome is caused by mutations in a putative sulphate transporter gene (PDS). Nat Genet 1997;17:411-422.

2 Choi BY, Muskett J, King KA, Zalewski CK, Shawker T, Reynolds JC, Butman JA, Brewer CC, Stewart AK, Alper SL, Griffith AJ: Hereditary hearing loss with thyroid abnormalities. Adv Otorhinolaryngol 2011;70:43-49.

3 Choi BY, Stewart AK, Madeo AC, Pryor SP, Lenhard S, Kittles R, Eisenman D, Kim HJ, Niparko J, Thomsen J, Arnos KS, Nance WE, King KA, Zalewski CK, Brewer CC, Shawker T, Reynolds JC, Butman JA, Karniski LP, Alper SL, Griffith AJ: Hypo-functional slc26a4 variants associated with nonsyndromic hearing loss and enlargement of the vestibular aqueduct: Genotype-phenotype correlation or coincidental polymorphisms? Hum Mutat 2009;30:599-608.

4 Dai P, Stewart AK, Chebib F, Hsu A, Rozenfeld J, Huang D, Kang D, Lip V, Fang H, Shao H, Liu X, Yu F, Yuan H, Kenna M, Miller DT, Shen Y, Yang W, Zelikovic I, Platt OS, Han D, Alper SL, Wu BL: Distinct and novel slc26a4/pendrin mutations in chinese and u.S. Patients with nonsyndromic hearing loss. Physiol Genom 2009;38:281-290.

5 Choi BY, Kim HM, Ito T, Lee KY, Li X, Monahan K, Wen Y, Wilson E, Kurima K, Saunders TL, Petralia RS, Wangemann P, Friedman TB, Griffith AJ: Mouse model of enlarged vestibular aqueducts defines temporal requirement of SLC26A4 expression for hearing acquisition. J Clin Invest 2011; in press.

6 Nakaya K, Harbidge DG, Wangemann P, Schultz BD, Green ED, Wall SM, Marcus DC: Lack of pendrin HCO_3^- transport elevates vestibular endolymphatic $[Ca^{2+}]$ by inhibition of acid-sensitive trpv5 and trpv6 channels. Am J Physiol Renal Physiol 2007;292:F1314-1321.

7 Wangemann P, Nakaya K, Wu T, Maganti RJ, Itza EM, Sanneman JD, Harbidge DG, Billings S, Marcus DC: Loss of cochlear HCO_3^- secretion causes deafness via endolymphatic acidification and inhibition of Ca^{2+} reabsorption in a pendred syndrome mouse model. Am J Physiol Renal Physiol 2007;292:F1345-1353.

8 Kim HM, Wangemann P: Failure of fluid absorption in the endolymphatic sac initiates cochlear enlargement that leads to deafness in mice lacking pendrin expression. PloS One 2010;5:e14041.

9 Gillam MP, Sidhaye AR, Lee EJ, Rutishauser J, Stephan CW, Kopp P: Functional characterization of pendrin in a polarized cell system. Evidence for pendrin-mediated apical iodide efflux. J Biol Chem 2004;279:13004-13010.

10 Royaux IE, Wall SM, Karniski LP, Everett LA, Suzuki K, Knepper MA, Green ED: Pendrin, encoded by the pendred syndrome gene, resides in the apical region of renal intercalated cells and mediates bicarbonate secretion. Proc Natl Acad Sci USA 2001;98:4221-4226.

11 Leviel F, Hubner CA, Houillier P, Morla L, El Moghrabi S, Brideau G, Hassan H, Parker MD, Kurth I, Kougioumtzes A, Sinning A, Pech V, Riemondy KA, Miller RL, Hummler E, Shull GE, Aronson PS, Doucet A, Wall SM, Chambrey R, Eladari D: The Na^+-dependent chloride-bicarbonate exchanger slc4a8 mediates an electroneutral Na^+ reabsorption process in the renal cortical collecting ducts of mice. J Clin Invest 2010;120:1627-1635.

12 Adler L, Efrati E, Zelikovic I: Molecular mechanisms of epithelial cell-specific expression and regulation of the human anion exchanger (pendrin) gene. Am J Physiol 2008;294:C1261-1276.

13 Rozenfeld J TO, Adler L, Efrati E, Stewart AK, Carrithers S, Alper SL, Zelikovic I: The pendrin gene is trancriptionally regulated by the intestinal natriuretic peptide, uroguanylin. Pediatr Nephrol 2010;25:A210.

14 Deyev IE, Sohet F, Vassilenko KP, Serova OV, Popova NV, Zozulya SA, Burova EB, Houillier P, Rzhevsky DI, Berchatova AA, Murashev AN, Chugunov AO, Efremov RG, Nikol'sky NN, Bertelli E, Eladari D, Petrenko AG: Insulin receptor-related receptor as an extracellular alkali sensor. Cell Metabol 2011;13:679-689.

15 Verlander JW, Hassell KA, Royaux IE, Glapion DM, Wang ME, Everett LA, Green ED, Wall SM: Deoxycorticosterone upregulates PDS (SLC26A4) in mouse kidney: Role of pendrin in mineralocorticoid-induced hypertension. Hypertension 2003;42:356-362.

16 Pech V, Pham TD, Hong S, Weinstein AM, Spencer KB, Duke BJ, Walp E, Kim YH, Sutliff RL, Bao HF, Eaton DC, Wall SM: Pendrin modulates ENaC function by changing luminal HCO_3^-. J Am Soc Nephrol 2010;21:1928-1941.

17 Kim YH, Pham TD, Zheng W, Hong S, Baylis C, Pech V, Beierwaltes WH, Farley DB, Braverman LE, Verlander JW, Wall SM: Role of pendrin in iodide balance: Going with the flow. Am J Physiol Renal Physiol 2009;297:F1069-1079.

18 Kandasamy N, Fugazzola L, Evans M, Chatterjee K, Karet F: Life-threatening metabolic alkalosis in pendred syndrome. Eur J Endocrinol 2011;165:167-170.

19 Pedemonte N, Caci E, Sondo E, Caputo A, Rhoden K, Pfeffer U, Di Candia M, Bandettini R, Ravazzolo R, Zegarra-Moran O, Galietta LJ: Thiocyanate transport in resting and IL-4-stimulated human bronchial epithelial cells: Role of pendrin and anion channels. J Immunol 2007;178:5144-5153.

20 Nakao I, Kanaji S, Ohta S, Matsushita H, Arima K, Yuyama N, Yamaya M, Nakayama K, Kubo H, Watanabe M, Sagara H, Sugiyama K, Tanaka H, Toda S, Hayashi H, Inoue H, Hoshino T, Shiraki A, Inoue M, Suzuki K, Aizawa H, Okinami S, Nagai H, Hasegawa M, Fukuda T, Green ED, Izuhara K: Identification of pendrin as a common mediator for mucus production in bronchial asthma and chronic obstructive pulmonary disease. J Immunol 2008;180:6262-6269.

21 Rillema JA, Hill MA: Pendrin transporter carries out iodide uptake into MCF-7 human mammary cancer cells. Exper Biol Med (Maywood, NJ) 2003;228:1078-1082.

22 Rillema JA, Hill MA: Prolactin regulation of the pendrin-iodide transporter in the mammary gland. Am J Physiol Endocrinol Metab 2003;284:E25-28.

23 Shcheynikov N, Yang D, Wang Y, Zeng W, Karniski LP, So I, Wall SM, Muallem S: The Slc26a4 transporter functions as an electroneutral Cl^-_i-/HCO_3- exchanger: Role of Slc26a4 and Slc26a6 in I- and HCO_3- secretion and in regulation of cftr in the parotid duct. J Physiol 2008;586:3813-3824.

24 Heneghan JF, Akhavein A, Salas MJ, Shmukler BE, Karniski LP, Vandorpe DH, Alper SL: Regulated transport of sulfate and oxalate by Slc26a2/Dtdst. Am J Physiol 2010;298:C1363-1375.

25 Chernova MN, Jiang L, Shmukler BE, Schweinfest CW, Blanco P, Freedman SD, Stewart AK, Alper SL: Acute regulation of the SLC26A3 congenital chloride diarrhoea anion exchanger (DRA) expressed in xenopus oocytes. J Physiol 2003;549:3-19.

26 Chernova MN, Jiang L, Friedman DJ, Darman RB, Lohi H, Kere J, Vandorpe DH, Alper SL: Functional comparison of mouse Slc26a6 anion exchanger with human SLC26A6 polypeptide variants: Differences in anion selectivity, regulation, and electrogenicity. J Biol Chem 2005;280:8564-8580.

27 Zhang Y, Chernova MN, Stuart-Tilley AK, Jiang L, Alper SL: The cytoplasmic and transmembrane domains of AE2 both contribute to regulation of anion exchange by pH. J Biol Chem 1996;271:5741-5749.

28 Ohno S, Akita Y, Konno Y, Imajoh S, Suzuki K: A novel phorbol ester receptor/protein kinase, nPKC, distantly related to the protein kinase C family. Cell 1988;53:731-741.

29 Hirai S, Izumi Y, Higa K, Kaibuchi K, Mizuno K, Osada S, Suzuki K, Ohno S: Ras-dependent signal transduction is indispensable but not sufficient for the activation of AP1/JUN by PKC delta. EMBO J 1994;13:2331-2340.

30 Takebe Y, Seiki M, Fujisawa J, Hoy P, Yokota K, Arai K, Yoshida M, Arai N: Sr alpha promoter: An efficient and versatile mammalian cDNA expression system composed of the simian virus 40 early promoter and the r-u5 segment of human t-cell leukemia virus type 1 long terminal repeat. Mol Cell Biol 1988;8:466-472.

31 Stewart AK, Kedar PS, Shmukler BE, Vandorpe DH, Hsu A, Glader B, Rivera A, Brugnara C, Alper SL: Functional characterization and modified rescue of novel AE1 mutation R730C associated with overhydrated cation leak stomatocytosis. Am J Physiol 2011;300:C1034-1046.

32 Stewart AK, Chernova MN, Shmukler BE, Wilhelm S, Alper SL: Regulation of AE2-mediated Cl^- transport by intracellular or by extracellular pH requires highly conserved amino acid residues of the AE2 NH2-terminal cytoplasmic domain. J Gen Physiol 2002;120:707-722.

33 Stewart AK, Chernova MN, Kunes YZ, Alper SL: Regulation of AE2 anion exchanger by intracellular pH: Critical regions of the NH(2)-terminal cytoplasmic domain. Am J Physiol 2001;281:C1344-1354.

34 Humphreys BD, Chernova MN, Jiang L, Zhang Y, Alper SL: NH_4Cl activates AE2 anion exchanger in xenopus oocytes at acidic pHi. Am J Physiol 1997;272:C1232-1240.

35 Scott DA, Karniski LP: Human pendrin expressed in xenopus laevis oocytes mediates chloride/formate exchange. Am J Physiol 2000;278:C207-211.

36 Dossena S, Vezzoli V, Cerutti N, Bazzini C, Tosco M, Sironi C, Rodighiero S, Meyer G, Fascio U, Furst J, Ritter M, Fugazzola L, Persani L, Zorowka P, Storelli C, Beck-Peccoz P, Botta G, Paulmichl M: Functional characterization of wild-type and a mutated form of SLC26A4 identified in a patient with pendred syndrome. Cell Physiol Biochem 2006;17:245-256.

37 Soleimani M, Greeley T, Petrovic S, Wang Z, Amlal H, Kopp P, Burnham CE: Pendrin: An apical $Cl^-/OH^-/HCO_3^-$ exchanger in the kidney cortex. Am J Physiol Renal Physiol 2001;280:F356-364.

38 Pera A, Dossena S, Rodighiero S, Gandia M, Botta G, Meyer G, Moreno F, Nofziger C, Hernandez-Chico C, Paulmichl M: Functional assessment of allelic variants in the SLC26A4 gene involved in pendred syndrome and nonsyndromic EVA. Proc Natl Acad Sci USA 2008;105:18608-18613.

39 Yoon JS, Park HJ, Yoo SY, Namkung W, Jo MJ, Koo SK, Park HY, Lee WS, Kim KH, Lee MG: Heterogeneity in the processing defect of SLC26A4 mutants. J Med Genet 2008;45:411-419.

40 Azroyan A, Laghmani K, Crambert G, Mordasini D, Doucet A, Edwards A: Regulation of pendrin by pH: Dependence on glycosylation. Biochem J 2011;434:61-72.

41 Dossena S, Rodighiero S, Vezzoli V, Bazzini C, Sironi C, Meyer G, Furst J, Ritter M, Garavaglia ML, Fugazzola L, Persani L, Zorowka P, Storelli C, Beck-Peccoz P, Botta G, Paulmichl M: Fast fluorometric method for measuring pendrin (SLC26A4) Cl^-/I^- transport activity. Cell Physiol Biochem 2006;18:67-74.

42 Emmons C: Transport characteristics of the apical anion exchanger of rabbit cortical collecting duct beta-cells. Am J Physiol1999;276:F635-643.

43 Shelden MC, Howitt SM, Price GD: Membrane topology of the cyanobacterial bicarbonate transporter, BicA, a member of the SulP (SLC26A) family. Mol Membr Biol 2011;27:12-23.

44 Clark JS, Vandorpe DH, Chernova MN, Heneghan JF, Stewart AK, Alper SL: Species differences in Cl^- affinity and in electrogenicity of Slc26a6-mediated oxalate/ Cl^- exchange correlate with the distinct human and mouse susceptibilities to nephrolithiasis. J Physiol 2008;586:1291-1306.

45 Hassan HA, Mentone S, Karniski LP, Rajendran VM, Aronson PS: Regulation of anion exchanger SLC26A6 by protein kinase C. Am J Physiol 2007;292:C1485-1492.

46 Bain J, Plater L, Elliott M, Shpiro N, Hastie CJ, McLauchlan H, Klevernic I, Arthur JS, Alessi DR, Cohen P: The selectivity of protein kinase inhibitors: A further update. Biochem J 2007;408:297-315.

47 Soltoff SP: Rottlerin is a mitochondrial uncoupler that decreases cellular atp levels and indirectly blocks protein kinase C delta tyrosine phosphorylation. J Biol Chem 2001;276:37986-37992.

48 Soltoff SP: Rottlerin: An inappropriate and ineffective inhibitor of PKC delta. Trends Pharmacol Sci 2007;28:453-458.

49 Zakharov SI, Morrow JP, Liu G, Yang L, Marx SO: Activation of the BK (Slo1) potassium channel by mallotoxin. J Biol Chem 2005;280:30882-30887.

50 Cohen P: Guidelines for the effective use of chemical inhibitors of protein function to understand their roles in cell regulation. Biochem J 2010;425:53-54.

51 Diamond JM, Wright EM: Biological membranes: The physical basis of ion and nonelectrolyte selectivity. Annu Rev Physiol 1969;31:581-646.

52 Krauss D, Eisenberg B, Gillespie D: Selectivity sequences in a model calcium channel: Role of electrostatic field strength. Eur Biophys J 2011;40:775-782.

53 Andersen OS: Perspectives on: Ion selectivity. J Gen Physiol 2011;137:393-395.

54 Emmons C: Halide transport patterns of apical anion exchange in rabbit cortical collecting duct intercalated cells. Am J Physiol 1996;271:F799-805.

55 Matsushima Y, Muto S, Taniguchi J, Imai M: Mechanism of iodide transport in the rabbit cortical collecting duct. Clin Exp Nephrol 2006;10:102-110.

56 Humphreys BD, Jiang L, Chernova MN, Alper SL: Functional characterization and regulation by pH of murine AE2 anion exchanger expressed in Xenopus oocytes. Am J Physiol 1994;267:C1295-1307.

57 Hunter MJ: Human erythrocyte anion permeabilities measured under conditions of net charge transfer. J Physiol 1977;268:35-49.

58 Parker MD, Young MT, Daly CM, Meech RW, Boron WF, Tanner MJ: A conductive pathway generated from fragments of the human red cell anion exchanger AE1. J Physiol 2007;581:33-50.

59 Dorwart MR, Shcheynikov N, Wang Y, Stippec S, Muallem S: Slc26a9 is a Cl^- channel regulated by the Wnk kinases. J Physiol 2007;584:333-345.

60 Kim KH, Shcheynikov N, Wang Y, Muallem S: SLC26A7 is a Cl^- channel regulated by intracellular pH. J Biol Chem 2005;280:6463-6470.

61 Dossena S, Maccagni A, Vezzoli V, Bazzini C, Garavaglia ML, Meyer G, Furst J, Ritter M, Fugazzola L, Persani L, Zorowka P, Storelli C, Beck-Peccoz P, Botta G, Paulmichl M: The expression of wild-type pendrin (SLC26A4) in human embryonic kidney (HEK 293 phoenix) cells leads to the activation of cationic currents. Eur J Endo 2005;153:693-699.

62 Yoshida A, Hisatome I, Taniguchi S, Sasaki N, Yamamoto Y, Miake J, Fukui H, Shimizu H, Okamura T, Okura T, Igawa O, Shigemasa C, Green ED, Kohn LD, Suzuki K: Mechanism of iodide/chloride exchange by pendrin. Endocrinology 2004;145:4301-4308.

63 Knauf PA, Pal P: Band 3 mediated transport; in Bernhardt I, Ellory, J.C. (eds): Red cell membrane transport in health and disease. Berlin, Springer, 2003, pp 253-301.

64 Scott DA, Wang R, Kreman TM, Sheffield VC, Karniski LP: The pendred syndrome gene encodes a chloride-iodide transport protein. Nat Genet 1999;21:440-443.

65 Garnett JP, Hickman E, Burrows R, Hegyi P, Tiszlavicz L, Cuthbert AW, Fong P, Gray MA: Novel role for pendrin in orchestrating bicarbonate secretion in CFTR-expressing airway serous cells. J Biol Chem 2011;in press.

66 Matulef K, Howery AE, Tan L, Kobertz WR, Du Bois J, Maduke M: Discovery of potent Clc chloride channel inhibitors. ACS Chem Biol 2008;3:419-428.

67 Simchowitz L, Davis AO: Intracellular pH recovery from alkalinization. Characterization of chloride and bicarbonate transport by the anion exchange system of human neutrophils. J Gen Physiol 1990;96:1037-1059.

68 Stewart AK, Shmukler BE, Vandorpe DH, Reimold F, Heneghan JF, Nakakuki M, Akhavein A, Ko S, Ishiguro H, Alper SL: Slc26 anion exchangers of guinea pig pancreatic duct: Molecular cloning and functional characterization. Am J Physiol 2011;301:C289-303.

69 Chernova MN, Jiang L, Crest M, Hand M, Vandorpe DH, Strange K, Alper SL: Electrogenic sulfate/chloride exchange in xenopus oocytes mediated by murine Ae1 E699Q. J Gen Physiol 1997;109:345-360.

70 Jennings ML: Rapid electrogenic sulfate-chloride exchange mediated by chemically modified band 3 in human erythrocytes. J Gen Physiol 1995;105:21-47.

71 Miller C, Nguitragool W: A provisional transport mechanism for a chloride channel-type Cl^-/H^+ exchanger. R Soc Lond Phil Trans 2009;364:175-180.

72 Ohana E, Shcheynikov N, Yang D, So I, Muallem S: Determinants of coupled transport and uncoupled current by the electrogenic SLC26 transporters. J Gen Physiol 2011;137:239-251.

73 Muscella A, Marsigliante S, Verri T, Urso L, Dimitri C, Botta G, Paulmichl M, Beck-Peccoz P, Fugazzola L, Storelli C: Pkc-epsilon-dependent cytosol-to-membrane translocation of pendrin in rat thyroid PC cl3 cells. J Cell Physiol 2008;217:103-112.

74 Chen L, Hahn H, Wu G, Chen CH, Liron T, Schechtman D, Cavallaro G, Banci L, Guo Y, Bolli R, Dorn GW, 2nd, Mochly-Rosen D: Opposing cardioprotective actions and parallel hypertrophic effects of delta PKC and epsilon PKC. Proc Natl Acad Sci USA 2001;98:11114-11119.

Cellular Physiology and Biochemistry

Erratum

Cell Physiol Biochem 2012;29:

In the article by Reimold et al. entitled “Pendrin Function and Regulation in *Xenopus* Oocytes” published in Cell Physiol Biochem 2011;28(3):435-450, Dr. Fabian R. Reimold, the co-first author of this publication, is also affiliated with: Department of Nephrology, Robert-Bosch-Krankenhaus, 70376 Stuttgart, Germany.

KARGER

Fax +41 61 306 12 34
E-Mail karger@karger.ch
www.karger.com

© 2012 S. Karger AG, Basel
1015-8987/12/0292-0000$38.00/0

Accessible online at:
www.karger.com/cpb